Available online at www.sciencedirect.com

ScienceDirect

Procedia Technology 22 (2016) 243 – 250

Procedia Technology

9th International Conference Interdisciplinarity in Engineering, INTER-ENG 2015, 8-9 October 2015, Tirgu-Mures, Romania

The Passive Mixing Phenomena in Microtubes with Baffle Configuration

Roxana Milotin[a], Dorin Lelea[a,*]

[a]*University Politehnica Timisoara, Faculty of Mechanical Engineering, Department of Thermal Machines and Transportation B-dul Mihai Viteazu nr. 1, 300222 Timisoara, Romania*

Abstract

The paper presents the analysis on passive mixing phenomena in microtubes considering three different configurations. Two of them having four baffles that create orifice with half and respectively quarter of the cross-section that are compared with the simple microtube. The micromixers have four inlet cross-sections with water and methanol as the working fluids. The mixing efficiency is evaluated through the mixing index that considers the standard deviation of the mass fraction at specific cross-section. Moreover the analysis is extended to Re = 0.2 – 91 in order to analyze the axial mixing length for each case considered. The analysis is performed numerically based on a finite volume code. It was concluded that best mixing results have the microtubes with orifices that occupy the quarter of the cross-section both for low Re and diffusion mixing or higher Re and mixing augmented by advection.

© 2016 The Authors. Published by Elsevier Ltd. This is an open access article under the CC BY-NC-ND license (http://creativecommons.org/licenses/by-nc-nd/4.0/).

Peer-review under responsibility of the "Petru Maior" University of Tirgu Mures, Faculty of Engineering

Keywords: micromixer; passive mixing; baffles; mixing index; mixing length.

1. Introduction

The micromixers are effective microfluidic tools with applications in various engineering fields as bioreactors, drug-delivery devices or μ-TAS. The proper design of micromixers implies the optimization of the hydrodynamic

* Corresponding author. Tel.: +40 256 403661;
E-mail address: dorin.lelea@upt.ro

2212-0173 © 2016 The Authors. Published by Elsevier Ltd. This is an open access article under the CC BY-NC-ND license (http://creativecommons.org/licenses/by-nc-nd/4.0/).
Peer-review under responsibility of the "Petru Maior" University of Tirgu Mures, Faculty of Engineering
doi:10.1016/j.protcy.2016.01.075

paths in order to obtain the compactness, uniform concentration and temperature of the mixture and short mixing length.

Nomenclature

b_1, m,	baffle length
b_2, m,	reservoir length
c, -,	mass fraction
D, m^2/s,	diffusion coefficient
D_i, m,	inner diameter
h, m,	inlet channel height
m, kg/s,	mass flow rate of the micromixer
M, -,	mixing index
n, -,	number of the sample points
p, Pa,	pressure
Re, -,	Reynolds number
s, m,	inlet channel width
u, v, w, m/s,	velocity components
x, y, z, m,	coordinate
Greek symbols	
μ, Pa s,	dynamic viscosity
ρ, kg/m^3,	density
σ, -,	standard deviation
Subscripts	
av,	average
max,	maximum

In the case of the passive mixing this might be obtained through increasing the contact area of the fluids, inducing instabilities or increasing the mixing path. Moreover the micromixers could attain more rapid and dynamic chemical reactions. Special attention is delivered to effective mixing in low Re regime due to incompatibility of the high shear rates and some biological species [1].

The passive mixing in microchannels was investigated both numerically and experimentally by various authors in last decade. Jeon and Shin [2] analyzed four different microfluidic configurations numerically and concluded that zig-zag has the best mixing efficiency at low Re. The results were also confirmed experimentally. Ansari et al. [3] investigated numerically the influence of the stream position on mixing phenomena in T-shape microchannels. It was found that stream position has more influence at low Re. Numerical analysis on microfluidic device with obstacles and alternate flow was analyzed by Miranda et al. [4]. Besides, the Σ-micromixer was analyzed and optimized by Tafti et al. [5]. Moreover, Afzal and Kim [6] optimized the micromixer with convergentdivergent sinusoidal walls considering both the mixing efficiency and pressure drop. The optimization was made for Re of 30. The analysis revealed significant variation in the ratio of throat width to depth of the convergent-divergent sections, whereas the ratio of amplitude to wavelength of the sinusoidal walls maintained a nearly constant value. Kleinstreuer et al. [7] investigated numerically the microfluidic device for nano-drug delivery. In the later report it is concluded that micromixer with baffles and injection unit with holes have better mixing efficiency of the nanoparticles and shorter mixing length than a simple T-shape configuration. The fundamental issues on chaotic mixing were analyzed numerically by Lin and Yang [8] revealing that interfacial area, that is continuously distorted and enlarged, increasing the fluid mixing. Lin et al. [9] analyzed numerically and experimentally the mixing phenomena in T-type micromixer enhanced by J–shaped baffles. It was found that percentage of mixing is increasing as the number of baffles and Re increases. The numerical and experimental investigation of rapid vortex micromixers was analyzed

by Long et al.[10]. Enhanced mixing is due to the larger interfacial contact area and fluid convection. Review analysis on passive micromixers was published by Hardt et al [11] for μ-TAS and microreactors, also by Mansur et al. [12] and Kumar et al. [13]. SAR μreactor was analyzed by Fang and Yang [14] while unsteady diffusion process in Y- shaped micromixers was analyzed by Broboana et al.[15]. Lin et al. [16] investigated rapid circular micromixer with unbalanced driving force. It was concluded that the rotational flow was established even at Re = 2.

Alam and Kim [17] analyzed numerically planar configuration of passive micromixer with circular chambers. Four different configurations were tested with Re = 0.1 – 100. It is observed that mixing performance is strongly dependent on micromixer configuration and Re. Also the proposed micromixer has excellent mixing performance at low Re but rather poor behaviour at Re > 50.

Modrea [18] presents the aspects on future developments in the field of nano and micro technology.

In this paper the mixing efficiency is evaluated for three different configurations: the basic one with four inlets positioned tangentially, one with four baffles that occupy half of the cross-section and micromixer with four baffles that create orifices that covers quarter of the cross-section. The mass flow rates cover the Re = 0.2 – 91 with water and methanol as the working fluids.

2. Numerical details

The passive mixing phenomena was analyzed, considering three different configurations of micromixers (Fig. 1). The first configuration is the basic one with four inlet channels (Fig. 1a), the second micromixer has four baffles that occupy half of the cross-section (Fig. 1b) and the third one has the orifices that occupy quarter of the cross-section and delayed 90^o counterclockwise (Fig. 1c). The geometry and the flow conditions are presented in Fig. 1d and table 1. In the case of the microchannels conventional theories are applicable to the microtubes with diameters down to 100 μm accordingly to Lelea etal [19].

Table 1. Geometry and flow conditions of the micromixers

L, cm	D, μm	b_1, μm	b_2, μm
1	300	100	300
s, μm	h, μm	m, kg/s	Re
75	200	10^{-8} – 4 10^{-6}	0.2 - 91

So the set of the Navier-Stokes equations can be used to analyze the present phenomena, as follows:
The conservation of mass:

$$\frac{\partial(\rho \cdot u_i)}{\partial x_i} = 0 \tag{1}$$

The conservation of momentum:

$$\frac{\partial(u_i \cdot \rho \cdot u_j)}{\partial x_i} = -\frac{\partial p}{\partial x_j} + \frac{\partial}{\partial x_i}\left(\mu \frac{\partial u_j}{\partial x_i}\right) \tag{2}$$

The conservation of species:

$$\frac{\partial(u_i \cdot C)}{\partial x_i} = \frac{\partial}{\partial x_i}\left(D \frac{\partial C}{\partial x_i}\right) \tag{3}$$

For the micromixers presented in this paper, the following boundary conditions are settled:
- The fluid flow is stationary, incompressible and laminar;
- The fluid properties of the water and methanol were considered constant with the values presented in table 2.
- The viscous dissipation is neglected because of the low flow rates;
- The uniform velocity field and the constant temperature are imposed at the channel inlet, while at the outlet the partial derivatives of the velocity and temperature in the streamwise direction are vanishing;
- The water was considered as Fluid 1 and methanol as Fluid 2, with inlet cross-sections presented in Fig. 1. Mass fraction is considered 1 at the methanol inlets and 0 for water inlets.

Table 2. Thermophysical properties of the water and methanol [20]

	Density (kg/m^3)	Diffusion coefficient (m^2/s)	Dynamic viscosity (Pa s)
Water	998.2	$1.6 \cdot 10^{-9}$	0.001003
Methanol	785	$1.6 \cdot 10^{-9}$	0.0005495

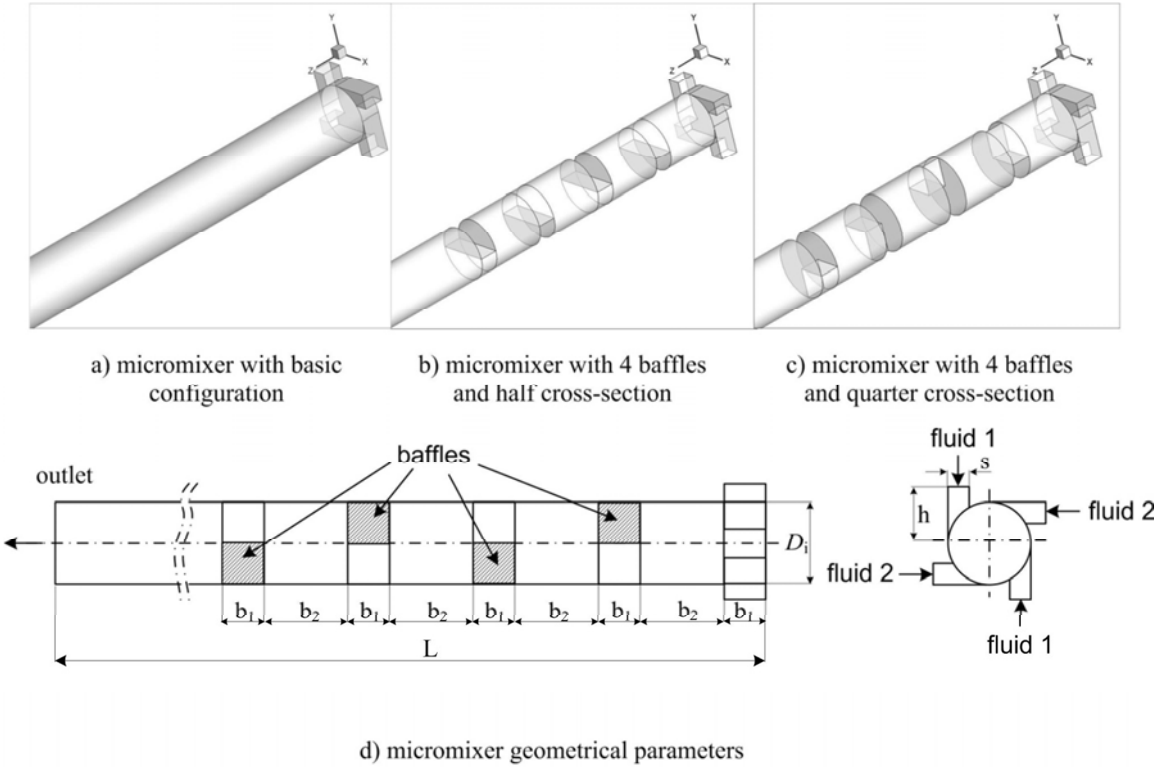

Fig. 1. The geometrical configuration of the micromixers

The set of the partial differential equations with boundary conditions are solved using the Ansys Fluent commercial solver [21] with methods described in [22]. The Simple algorithm is used for the velocity-pressure coupling solution and QUICK scheme for discretization of the partial differential equations for momentum and concentration species. The under-relaxation factors are used for pressure field ($\alpha = 0.3$), momentum conservation ($\alpha = 0.5$) and species conservation ($\alpha = 0.8$). The convergence criterion is defined as:

$$R^{\phi} = \frac{\sum_{cells,P} \left| \sum_{nb} a_{nb} \cdot \phi_{nb} + b - a_p \phi_p \right|}{\sum_{cells,P} \left| a_p \phi_p \right|} \tag{4}$$

The residuals for velocity components, continuity equation and concentration field were 10^{-8}. Three different quasi-structured grids have been used to test the grid sensitivity for the case with four baffles that covers quarter of the cross-section. Mesh 1 with total of 0.35 million cells, Mesh 2 with total of 0.8 million cells and Mesh 3 with 1.3 million cells. In Fig. 2 the mixing index distribution is presented for these three grids and Re = 45. A difference between grids nr. 2 and 3 is lower than 0.1 % so the mesh nr. 2 is used for further calculations. Moreover the validation of the numerical model for tangential injection of the fluid into the microtubes is presented in Lelea [23].

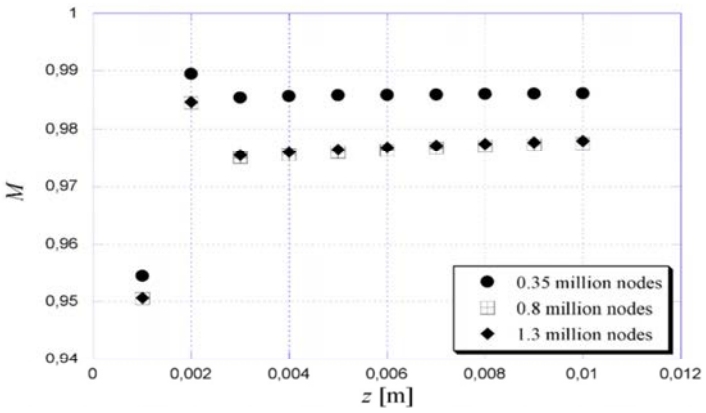

Fig. 2. The grid sensitivity analysis

3. Results and discussion

The mixing behaviour in microtubes for three different configurations was evaluated in terms of mixing index defined with the following equation:

$$M = 1 - \sqrt{\frac{\sigma^2}{\sigma_{max}^2}} \tag{5}$$

where the standard deviation of the mass fraction was calculated at specific cross-sections with the following relation:

$$\sigma = \sqrt{\frac{\sum_{i=1}^{n} (c_i - c_{av})^2}{n}} \tag{6}$$

the c_{av} is the average of the mass fraction c_i at specific cross-section defined with the following relation:

$$c_{av} = \frac{\sum_{i=1}^{n} c_i}{n} \tag{7}$$

Besides, Re is calculated with the following relation:

$$Re = \frac{\rho \cdot u_{av} \cdot D_i}{\mu} \tag{8}$$

The mixing index at the outlet cross section versus Re for three different configurations is presented in Fig. 3. It is concluded that mixing index is decreasing with Re for all configurations attaining the minimum value at Re ≅ 15. For very low Re the mixing phenomena is realizing through molecular diffusion obviously with higher residence time that increases mixing efficiency. Moreover the contact area between mixing fluids is higher due to four inlet jets. Besides, the mixing efficiency is higher for orifices that cover quarter of the cross-section, followed by the orifices covering half of the cross-section and finally the basic configuration. The reason for this might be explained by higher residence time in the case of the micrtubes with baffles. Moreover in the case of the micromixers with baffles the mixing index does not decrease linearly in the initial phase. As it is expected the minimum mixing index is $M = 0.36$ for basic configuration, $M = 0.48$ for half baffles and $M = 0.74$ for quarter baffles.

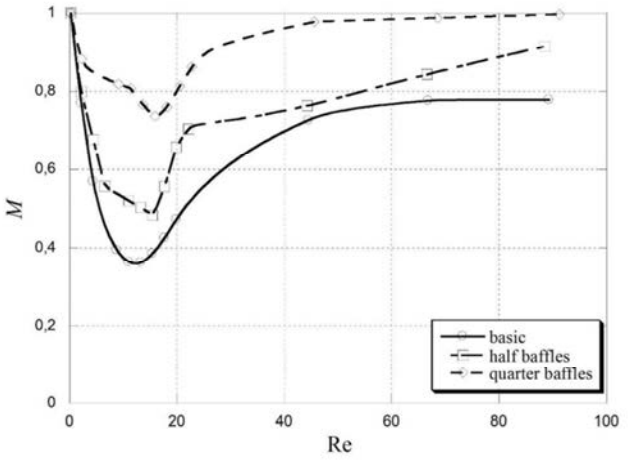

Fig. 3. The mixing index versus Re

Following the minimum point of the mixing index distribution, it increases for all considered configurations. In the case of the micromixer without the baffles the mixing index is approaching $M = 0.77$ at Re = 60. The mixing index for micromixer with four baffles that covers the half cross-section has two distinct phases. In the first one the mixing index increases abruptly until Re = 22 followed by the relatively slowly increasing mixing efficiency. The maximum $M = 0.91$ is obtained for approximately Re = 90. In the case of the micromixer with four baffles that covers the quarter of the cross-section the mixing index attains very rapidly $M \cong 1$ at Re ≅ 40.

In Figs. 4a – 4c the axial distribution of the mixing index is presented for three different configurations and various Re. It is observed that mixing efficiency increases with axial distance regardless the configuration or Re. For basic configuration (Fig. 4a) the mixing index is monotonically increasing for all Re. Except for very low Re = 2 and 4, a mixing index range is the same for the rest of the cases.

In Fig. 4b the mixing index distribution is presented for micromixer with half baffles. It is observed that intense mixing is obtained in the entrance region with the baffles even for low Re = 2 and 4. For $z > 2$ mm the mixing index constantly increases with the same rate for all Re. For Re > 40 the complete swirl motion is established in the micromixer due to tangential position of the inlet cross-sections so the sharp increase in mixing efficiency is observed. Moreover for the latter case the mixing efficiency remains almost constant after the baffle zone.

If the orifices created by the baffles that covers only the quarter of the cross-section and delayed for 90^o (Fig. 4c), the longer contact path between the fluids and higher residence time is obtained. Moreover due to the fact that the orifices are delayed the rotational motion is obtained even for low Re. Consequently the rapid mixing is obtained

in the initial region with baffles for all the cases considered. Moreover for Re > 45 the fluids are almost completely mixed ($M > 0.95$) after $z = 1$ mm.

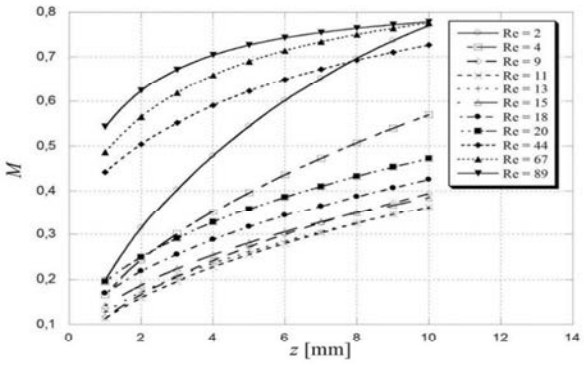

a) basic configuration

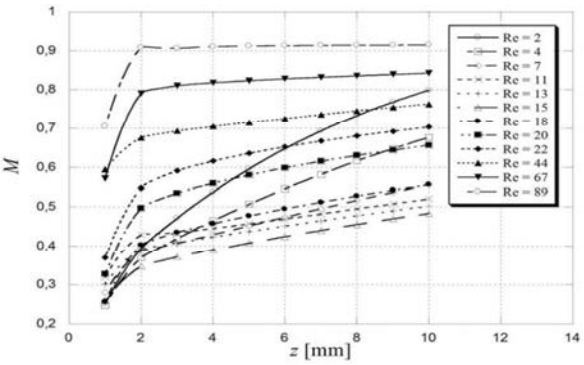

b) half baffles

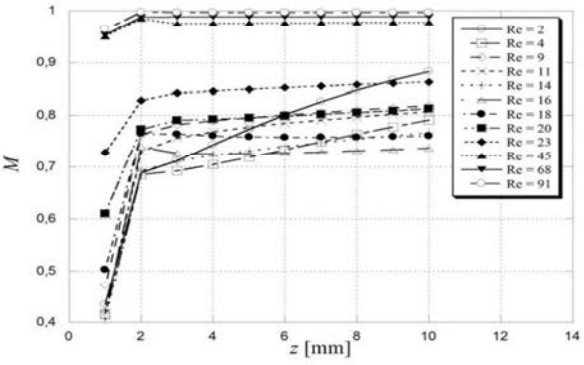

c) quarter baffles

Fig. 4. The axial distribution of the mixing index for three different configurations

4. Conclusions

The analysis regarding the mixing efficiency of the micromixer with three different configurations was made: basic configurations with bare microtube, micromixer with four baffles that covers the half of the cross-section and micromixer with baffles that creates the orifice covering the quarter of the cross-section. The following conclusions are outlined:

-The hydrodynamic conditions strongly influence the mixing efficiency.

-The four inlet jets increase the contact area and at higher Re generate the swirl flow resulting in better mixing.

-The configurations with baffles that create the orifice on the quarter of the cross-section has the superior mixing index with minimum M = 0.74 and maximum M = 1. The main reason for this is that delayed orifices create the rotational flow conditions regarding the Re. Moreover the flow instabilities are observed even for low Re.

-Based on the conclusions obtained from the numerical research, new configurations for micro-mixers used for nanodrug delivery might be considered.

Acknowledgements

The paper was partially supported by *Politehnica University Timisoara* Grant support program.

References

[1] Nguyen NT. Micromixers-Fundamentals, Design and Fabrication. William Andrew; 2008.
[2] Jeon W, Shin CB. Design and simulation of passive mixing in microfluidic systems with geometric variations. Chem. Eng. J 2009; 152: 575 – 582.
[3] Ansari MA, Kim KY, Kim SM. Numerical study of the effect on mixing of the position of fluid stream interfaces in a rectangular microchannel. Microsyst Technol 2010; 16: 1757–1763.
[4] Miranda JM, Oliveira H, Teixeira JA, Vicente AA, Correia JH, Minas G. Numerical study of micromixing combining alternate flow and obstacles. Int Commun Heat Mass 2010; 37: 581–586.
[5] Tafti EY, Kumar R, Cho HJ. Diffusive mixing through velocity profilevariation in microchannels. Exp Fluids 2011; 50: 535–545.
[6] Afzal A, Kim KY. Multi-Objective Optimization of a Micromixer with Convergent-Divergent Sinusoidal Walls. Chem Eng Commun. doi: 10.1080/00986445.2014.935352.
[7] Kleinstreuer C, Li J, Koo J. Microfluidics of nano-drug delivery. Int J Heat Mass Tran 2008; 51: 5590–5597.
[8] Lin KW, Yang JT. Chaotic mixing of fluids in a planar serpentine channel. Int J Heat Mass Tran 2007; 50: 1269–1277.
[9] Lin YC, Chung YC, Wu CY. Mixing enhancement of the passive microfluidic mixer with J-shaped baffles in the tee channel. Biomed Microdevices 2007; 9: 215–221.
[10] Long M, Sprague MA, Grimes AA, Rich BD, Khine M. A simple three-dimensional vortex micromixer. Appl Phys Lett 2009; 94: 133501.
[11] Hardt S, Drese KS, Hessel V, Schonfeld F. Passive micromixers for applications in the microreactor and μ-TAS fields. Microfluid Nanofluid 2005; 1: 108–118.
[12] Mansur EA, Mingxing YE, Yundong W, Youyuan D. A State-of-the-Art Review of Mixing in Microfluidic Mixers. Chinese J Chem Eng 2008; 16 (4): 503 - 516.
[13] Kumar V, Paraschivoiu M, Nigam KDP. Single-phase fluid flow and mixing in microchannels. Chem Eng Sci 2011; 66: 1329–1373.
[14] Fang WF, Yang JT. A novel microreactor with 3D rotating flow to boost fluid reaction and mixing of viscous fluids. Sensor Actuat B-Chem 2009; 140: 629–642.
[15] Broboana D, Balan CM, Wohland T, Balan C. Investigations of the unsteady diffusion process in microchannels. Chem Eng Sci 2011; 66: 1962–1972.
[16] Lin CH, Tsai CH, Pan CW, Fu LM. Rapid circular microfluidic mixer utilizing unbalanced driving force. Biomed Microdevices 2007; 9: 43–50.
[17] Alam A, Kim KY. Mixing performance of a planar micromixer with circular chambers and crossing constriction channels. Sensor Actuat B-Chem 2013; 176: 639– 652.
[18] Modrea A. Strategy for the future in terms of research and development in the field of nano and microtechnology. Procedia Technology 2014; 19: 283-288.
[19] Lelea D, Nishio S, Takano K. The experimental research on microtube heat transfer and fluid flow of distilled water. Int J Heat Mass Tran 2004; 47: 2817-2830.
[20] Perry R, Green D. Perry's Chemical Engineers' Handbook, McGraw-Hill, New York, NY, 1999.
[21] Ansys Fluent 14.0 documentation. Ansys Inc; 2011.
[22] Patankar SV. Numerical Heat Transfer and Fluid Flow. McGraw Hill –New York; 1980.
[23] Lelea D. Effects of inlet geometry on heat transfer and fluid flow of tangential micro-heat sink. Int J Heat Mass Tran 2010; 53: 3562–3569.